Photoelectric Characteristics of Nanocrystalline TiO_2 Film Prepared from TiO_2 Colloid Sol for Dye-Sensitized Solar Cell

Kyung-Jun Hwang, Jae-Wook Lee, Ho-Sung Yoon,† Hee-Dong Jang,† Jin-Geol Kim,‡ Jin Suk Yang,§ and Seung-Joon Yoo#,*

Department of Chemical and Biochemical Engineering, Chosun University, Gwangju 501-759, Korea
†Korea Institute of Geoscience and Mineral Resources, Daejeon 305-350, Korea
‡Department of Chemical Engineering, Soonchunhyang University, Asan, Chungnam 561-756, Korea
§Department of Chemical and Biomolecular Engineering, Sogang University, 1, Sinsoo, Seoul 121-742, Korea
#Department of Environmental and Chemical Engineering, Seonam University, Namwon 590-711, Korea
**E-mail: sjyoo001@hanmail.net*
Received May 13, 2009, Accepted September 1, 2009

A working electrode in dye-sensitized solar cells was fabricated using TiO_2 colloidal sol prepared from titanium isopropoxide used as a starting material by applying the sol-gel method. The effect of aging times and temperatures on physical and chemical properties of TiO_2 sol particles was systematically investigated. Results showed that the crystallinity and average particle size of TiO_2 colloidal sol can be successfully controlled by the adjustment of aging time and temperature. The conversion efficiency of the repetitive dry coating films fabricated using the dried TiO_2 colloidal sol particles and hydroxypropyl cellulose binder (15%) was 10.31% with a high transparency.

Key Words: Dye-sensitized solar cell, TiO_2 colloidal sol, Aging

Introduction

Dye-sensitized solar cells (DSSCs) are the most promising alternative to conventional solar cells conceived in recent years.[1] Nanosized TiO_2 particles have received great attention for use as a photoelectrode in dye-sensitized solar cell systems. In general, the TiO_2 photoelectrode consists of nanosized colloids that are sintered on a transparent conducting substrate, thus having a porous geometry.[2,3] Various preparation methods such as soft chemistry, hydrothermal, and the sol-gel process have been suggested for nanosized TiO_2 colloids.[4-6] It has been reported that the sol-gel process has many advantages for the fabrication of thin film in DSSC. The function of nanocrystalline thin films fabricated from colloidal sol has been found to be strongly dependent on the sol preparation process. Such synthetic procedures have been shown to control a wide range of material properties of the resulting films, in including particle size and crystallographic phase, film porosity, surface structure, electron transport properties, and optical light scattering.[7] Recently, the synthesis of TiO_2 colloidal paste for making of photoelectrode in DSSCs is much attention from all over the world.[8] Unfortunately, there is no report on the systematic controls of microstructured TiO_2 thin film to induce a high efficiency of DSSCs up to now.

In this study, the effect of aging conditions in the TiO_2 sol preparation was investigated to make TiO_2 thin film having a high transparency and a high efficiency in DSSCs. For the control of nanostructured TiO_2 thin films, TiO_2 colloidal sol was prepared through the aging process accompanied by hydrolysis/polycondensation using titanium-tetraisopropoxide (TTIP) as a starting material. We found that the aging process among the sol preparation steps is the most important step in controlling the size and structure of TiO_2 colloidal sol. We also found that the performance of DSSC using the resultant TiO_2 film is highly affected by the physical and chemical properties of TiO_2 sol particles.

Experimental

Synthesis of TiO_2 colloidal sols (i.e., SN-TiO_2 sol). Figure 1 shows a schematic diagram for the synthesis of TiO_2 sol and particles from a starting material. The reaction between TTIP (Titanium tetra-isopropoxide, Junsei Chemical Co. > 98%) and H_2O was performed under the condition of 1000 rpm and temperatures of 40 °C and 90 °C. The amount of water was fixed at 100 H_2O/Ti molar ratio.[9] The first chemical reaction was a hydrolysis between TTIP and water and it was too fast to control the reaction rate. On the other hand, after the initial hydrolysis, the reaction was easily controlled because of the slow rate. The characteristic of TiO_2 sol particles was controlled by optimizing the time and temperature of aging. The initial fast reaction between the water and TTIP reached the equilibrium temperature within 30 min. The reaction after 30 min was named "aging". The effect of aging was investigated according to the variation of aging times (0, 24, 72 h) under the condition of two different aging temperatures of 40 °C and 90 °C. The characteristics of TiO_2 sol particles was measured by the effect of the aging time under the condition of aging temperatures with 40 °C and 90 °C and a mixing rate of 1000 rpm. After the aging, TiO_2 solution was transformed into a solution phase like paste, and a peptizing agent needed acidic or basic electrolyte to peptize the solution effectively. Although various electrolytes such as HCl, HNO_3 and NH_4OH were available for peptizing agent, this experiment was performed under the condition of HCl to derive the ionic repulsive force required at the condition of low concentration. An acidic electrolyte was

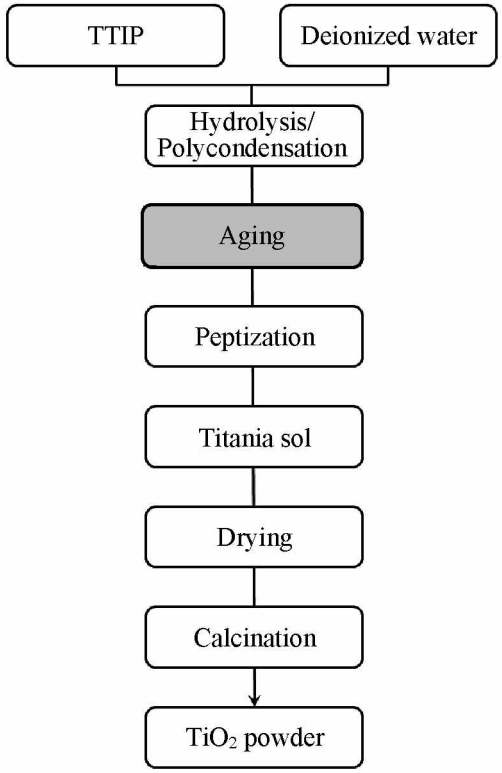

Figure 1. Experimental flowchart for the synthesis of TiO_2.

added in the solution with TiO_2 aggregated particles determined by aging to induce the repulsive force of interparticles and prevent continuous aggregation. At this point, the acidic electrolyte was selected with a nitric acid (HNO_3, Daejung Co. 60%) as an inorganic acid. The amount of the HNO_3 was optimized at 0.25 HNO_3/Ti molar ratio condition determined by the preliminary experiment. The hydrous TiO_2 sol was dried at 80 °C for 1 day and calcined at 500 °C by 2 °C/min for 1 hr at the final temperature to obtain a photoelectrode thin film.

Preparation of TiO_2 thin film. As mentioned before, SN-TiO_2 powders were obtained under the variation of aging times (0, 24, 72 h) at two different aging temperatures (40 °C and 90 °C). For the TiO_2 thin film, TiO_2 slurry was prepared by mixing of 2 g SN-TiO_2 particles, 0.68 mL 10% [V/V] acetyl acetone, 1 g hydroxypropyl cellulose (i.e., HPC, Mw. 80,000, Aldrich), and 10.68 mL water for 30 min at 300 rpm using a paste mixer (PDM-300, Korea mixing technology Co.). Thus, SN-TiO_2 film was fabricated by coating blended paste onto the fluorine-doped SnO_2 conducting glass plates (FTO, 10 Ω/cm^2, Asahi glass Co.) using a squeeze printing technique (adhesive tape was used as spacer of *ca.* 65 μm thickness. The TiO_2 film was heat-treated at 500 °C for 1 h. The TiO_2 film formed on the FTO glass was 7 μm thick and 0.5 cm × 0.5 cm. The TiO_2 thin film was prepared under the different mixing ratio of the dried SN-TiO_2 (5 ~ 25 wt%) and HPC binder (10 ~ 25 wt%) for photoelectrode with high efficiency and high transparency. In addition, repetitive dry coating of the TiO_2 film was conducted to enhance the conversion efficiency of DSSCs.[10]

To fabricate the DSSCs, the prepared TiO_2 thin film electrode was immersed in the N719 dye (Solaronix Co.) solution of 5 × 10^{-4} M at 50 °C for 4 h, rinsed with anhydrous ethanol and dried. A Pt coated glass-SnO_2: F (FTO, 10 Ω/cm^2, Asahi glass Co.) electrode was prepared as a counter electrode with an active area of 0.25 cm^2. The Pt electrode was placed over the dye-adsorbed TiO_2 thin film electrode, and the edges of the cell were sealed with 5 mm wide stripers of 60 μm thick sealing sheet (SX 1170-60, Solaronix). Sealing was accomplished by hot-pressing the two electrodes together at 120 °C. The redox electrolyte was injected into the cell through the small holes and sealed with a small square of sealing sheet. The redox electrolyte consists of 0.3 M 1,2-dimethyl-3-propylimidazolium iodide (Solaronix), 0.5 M LiI (Aldrich), 0.05 M I_2 (Aldrich), and 0.5 M 4-tert-butylpyridine (4-TBP, Aldrich) and 3-metoxypropionitrile nitrile (3-MPN, Fluka) as a solvent.

Characterization of SN-TiO_2 sol and SN-TiO_2 thin film. To investigate to change in crystallinity caused by aging conditon, the crystallinity of the manufactured SN-TiO_2 powder was characterized by an X-ray diffraction (Rigaku, D/MAX-1200) using a Cu $k\alpha$ X-ray and Ni filter at 35 kV and 15 mA. In addition, to probe the particle size and formation process of TiO_2 sol particle, the dried TiO_2 sol powders were investigated by transmission electron microscopy (HR-TEM, TECNAI, F20). Moreover, the Fourier transform infrared spectrophotometer (FT-IR, Jasco, FT/IR-410) was used to analyze microstructure changes in SN-TiO_2 particle cause by aging conditions. The thickness and surface morphology of TiO_2 thin film prepared from dried SN-TiO_2 as well as the calcined SN-TiO_2 were measured by field-emission scanning electron microscopy (FE-SEM, S-4700, Hitachi). The capacities of fabricated DSSCs and the current-voltage (*I-V*) curves were measured using a source measure unit under irradiation of white light from a 1000 W Xenon lamp (Thermo Oriel Instruments, USA). The incident light intensity and the active cell area were 100 mW/cm^2 and 0.25 cm^2, respectively. The *I-V* curves were used to calculate the short-circuit current (I_{sc}), open-circuit voltage (V_{oc}), fill factor (*FF*), and overall conversion efficiency (η_{eff}) of DSSCs. Thus, the electrochemical impedance spectroscopy (EIS) measurements were performed using the AC impedance (CHI 660A Electrochemical Workstation, USA) over the frequency ranging from 1 to 10^6 Hz with amplitudes of ± 5 mV over the V_{oc}.

Results and Discussion

Characterization of SN-TiO_2 sol particles and SN-TiO_2 thin film. Figures 2 (a) ~ (f) show HR-TEM images of SN-TiO_2 sol particles prepared under different aging times at two temperatures. Figures 2 (a) ~ (c) present the sizes and shapes of sol particles according to the aging times (0, 24, 72 h) at lower 40 °C. At 0 h, TiO_2 sol particles are 3 ~ 5 nm like a primary particle. On the other hand, after 24 h, sol particles are aggregated to large particles. Finally, after 72 h, particles are necked and aggregated to the structure of a bunch of grapes. Figures 2 (d) ~ (f) show the aggregated particles under the aging temperature of higher 90 °C. At 0 h, many sol particles are aggregated to larger bunches of grapes than in the case of Figure 1 (c).[11,12] After 72 h at 90 °C, the average particle size aggregated is about 50 nm showing the formation of continuous necking of

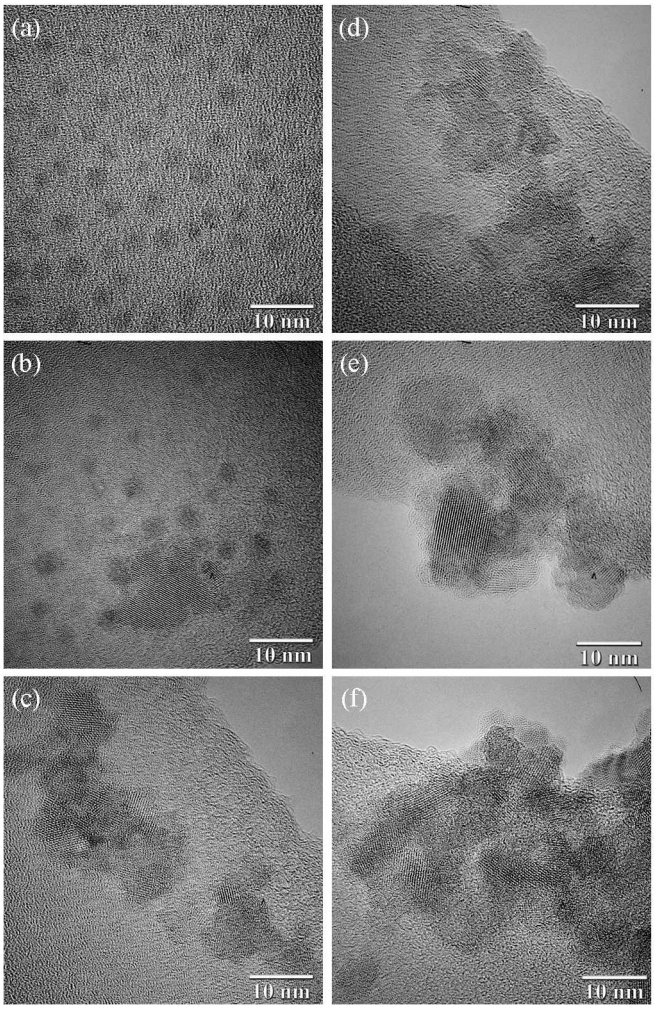

Figure 2. HR-TEM image of SN-TiO_2 sol particles according to the aging times (0 h (a,d), 24 h (b,e) and 72 h (c,f)) at 40 °C (left side) and at 90 °C (right side).

primary sol particles. These findings led us to conclude that aging temperatures rather than aging times are promoting the aggregation of particles. In the case of 72 h at 90 °C (right side), however, the particle size was the biggest, the color of TiO_2 sol was opaque, and the viscosity increased more than in the case of 0 h at 40 °C. We found from this result that the aging time and temperature are important process variables in controlling the size particle size. The crystallinity of TiO_2 sol particles and calcined TiO_2 particles was analyzed by XRD. Figures 3 (a, b) show the XRD patterns of dried TiO_2 sol prepared under different aging times at two different temperatures of at 40 °C and 90 °C. Before calcination, all samples had the brookite crystalline phase mainly. With increasing aging times at 40 °C, an increment in the brookite crystalline phase was observed. Also, TiO_2 sol prepared at 72 h and 90 °C (Figure 3 (b)) shows an intensity brookite peak at 25° higher than that of the TiO_2 sol prepared at 72 h and 40 °C (Figure 3 (a)). It may be safe to conclude that the crystallinity increased with the aging temperatures and times. In addition, the XRD patterns of calcined SN-TiO_2 (500 °C) particles prepared under different aging conditions were investigated. Numerous changes were observed with the aging times for the sample of 40 °C (Figure 2 (c)). With increasing aging times, TiO_2 particles having rutile crystalline phase as (110) were changed into anatase crystalline phase as (101). For the sample of 72 h, a greater amount of rutile phase changed to an anatase crystalline phase with the small existence of brookite crystalline phase (121) and also small rutile crystalline phase as (110). However, anatase crystalline phases for the samples (24 h, 72 h) at 90 °C was observed mosltly (Figure 3 (d)). Figure 4 shows the result of FT-infrared spectra (FT-IR) for different aging temperatures of 40 °C and 90 °C. The type and the amount of bonding group existing in the dried TiO_2 sol particles were analyzed using the KBr method in the range of 400 to 4,000 cm^{-1} wavelength number. In general, the characteristic absorption peaks of Ti-O-bending vibration and Ti-OH stretching vibration in the dried TiO_2 sol particles appear at 500 cm^{-1} and 1,630 cm^{-1}. As expected, the unique vibration peak of Ti-O-bending and Ti-OH stretching was observed as shown in Figure 4, and the intensity of Ti-O-absorption peak near 500 cm^{-1} increased with the progression of aging. In the result of FT-IR as shown Figure 4 (a), Ti-OH groups are largely formed with the progression of aging, and then they turn into Ti-O-Ti bond from Ti-OH bonds by polymerization/condensation as follows; Ti-OH + Ti-OH → Ti-O-Ti + H_2O.

On the other hand, all the chemical bonds reach the equilibrium state in the case of the aging of 72 h. Even though there is no chemical change anymore, the particles are aggregated by physical bonds according to aging. As a result, crystalline phases are affected by particle size even the calcinations of 500 °C as shown in Figure 3 (c, d). Therefore, the bigger the particle sizes, the slower the transition of the crystalline phase. Thus, the aging is an important process for the increase of particle size irrespective of chemical or physical processes.

Photoelectric characteristics of SN-TiO_2 films. The properties of the nanostructured TiO_2 particle synthesized in this work were investigated to prepare for feasible DSSCs. The role of aging condition in the making of photoelectrode for DSSCs was assessed on the basic of photovoltaic performance. Figure 5 shows the FE-SEM images of calcined SN-TiO_2 thin films. In the case of the samples of different aging times (a, c) for 0 h, rutile phase with big particle size (> 50 nm) was mostly observed after calcination at 500 °C. On the other hand, in the case of 72 h (b, d), anatase phase with small particle size (av. 20 nm) was mostly observed under the same calcination temperature of 500 °C. An examination of the photovoltaic performance of calcined SN-TiO_2 particle films with respect to their aging conditions revealed the current density (J_{sc}), open circuit voltage (V_{oc}), fill factor (FF), and energy conversion efficiency (η_{eff}) as summarized in

Table 1. When the aging times of 0 h and 72 h at 40 °C are compared, the sample of 0 h gave a low current density because of its amount of rutile crystalline phase relatively larger than the anatase phase. This may be attributed to the fact that the dye adsorption capacity of the photoelectrode consisting of high rutile crystalline was lower than that of high anatase crystalline. Thus, the high current density of photoelectrode was noted in the case of the sample having high anatase crystalline phase.[13-15] With increasing aging temperature, the efficiency increased from 3.96% to 4.63% under the same aging time of

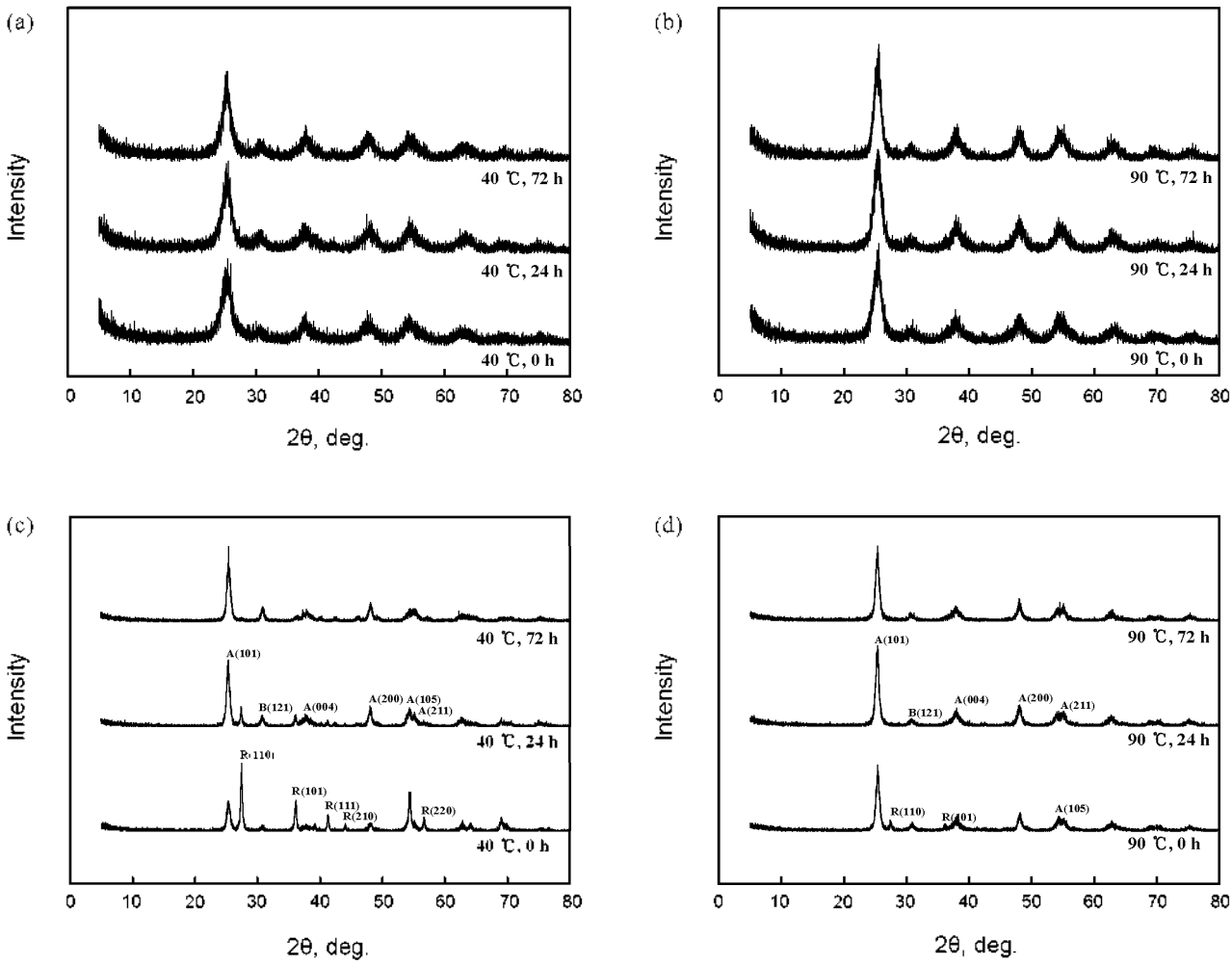

Figure 3. XRD patterns of dried SN-TiO_2 sol particles (above) and calcined SN-TiO_2 sol particles (bellow) with various aging time at 40 °C (a,c) and at 90 °C (b,d).

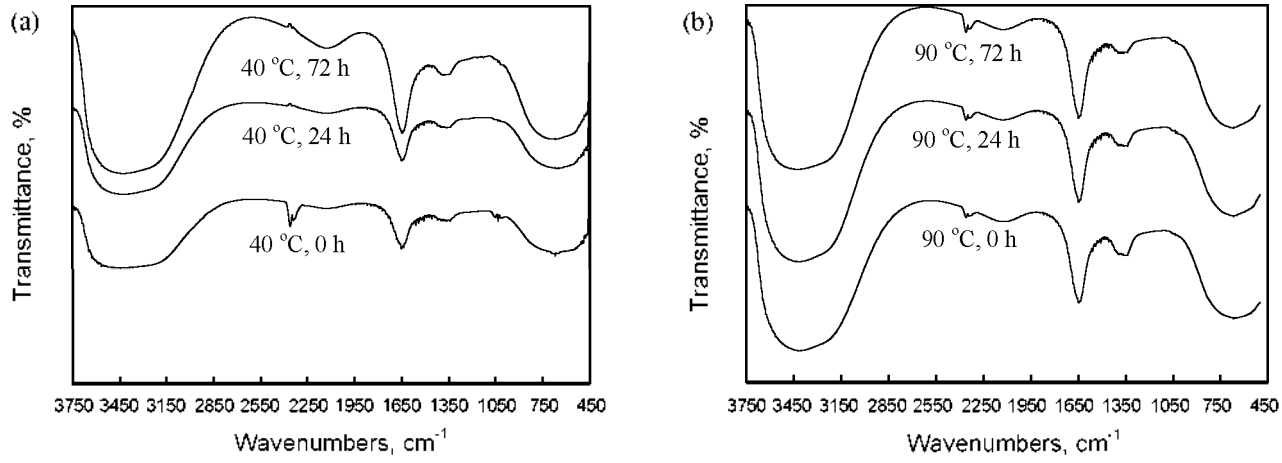

Figure 4. FT-IR spectra of dried SN-TiO_2 sol particles with various aging time at 40 °C (a) and at 90 °C (b).

72 h. Figure 6 shows the Nyquist plots of calcined SN-TiO_2 thin film with different aging times at 40 °C. A large semi-circle at low frequencies and a small one at high frequencies were observed for three solar cells. Responses in the frequency regions $10^3 \sim 10^6$, $1 \sim 10^3$, and $0.1 \sim 1$ Hz are assigned to charge transfer processes occurring at the Pt/electrolyte interface and TiO_2/dye/electrolyte interface, in Nernst diffusion within the electrolyte, respectively. The resistance at the TiO_2/dye/elec-

Table 1. Photocurrent-voltage of DSSCs for calcined SN-TiO_2 thin films under different aging times at 40 °C and 90 °C.

Type of temperature	Aging time	I_{sc}, mA/cm^2	V_{oc}, V	Fill factor, *FF*	η_{eff}, %
40 °C	0 h	6.68	0.64	0.62	2.64
	24 h	10.01	0.64	0.62	3.94
	72 h	10.32	0.63	0.61	3.96
90 °C	0 h	10.63	0.62	0.55	3.66
	24 h	12.56	0.60	0.54	4.06
	72 h	12.77	0.62	0.59	4.63

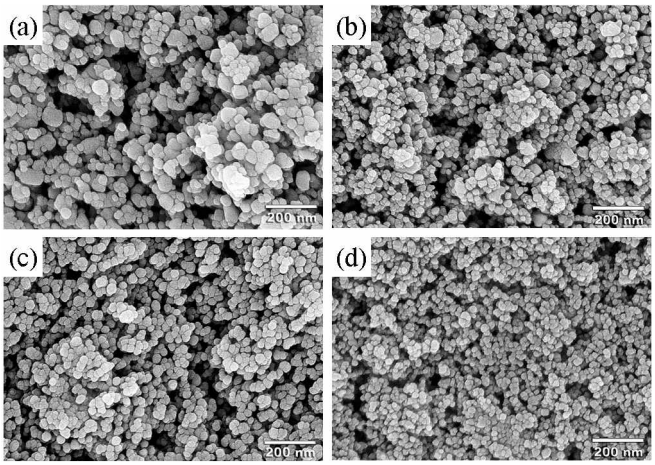

Figure 5. FE-SEM image of calcined SN-TiO_2 thin films with aging times (0 h (a,c) and 72 h (b,d)) at 40 °C (upside) and at 90 °C (downside).

Table 2. Photocurrent-voltage of DSSCs using dried SN-TiO_2 thin films depending on TiO_2 content.

TiO_2 content in the paste	I_{sc}, mA/cm^2	V_{oc}, V	Fill factor, *FF*	η_{eff}, %
5% SN-TiO_2	5.61	0.62	0.63	2.19
10% SN-TiO_2	8.56	0.63	0.63	3.41
15% SN-TiO_2	11.81	0.63	0.62	4.58
20% SN-TiO_2	14.15	0.64	0.57	5.16
25% SN-TiO_2	8.18	0.63	0.63	3.24

Table 3. Photocurrent-voltage of DSSCs using dried SN-TiO_2 thin films depending on HPC binder concentrations.

HPC concentration in the paste	I_{sc}, mA/cm^2	V_{oc}, V	Fill factor, *FF*	η_{eff}, %
10% HPC	16.33	0.67	0.59	6.46
15% HPC	17.69	0.70	0.62	7.80
20% HPC	13.95	0.65	0.66	5.98
25% HPC	10.16	0.63	0.66	4.20

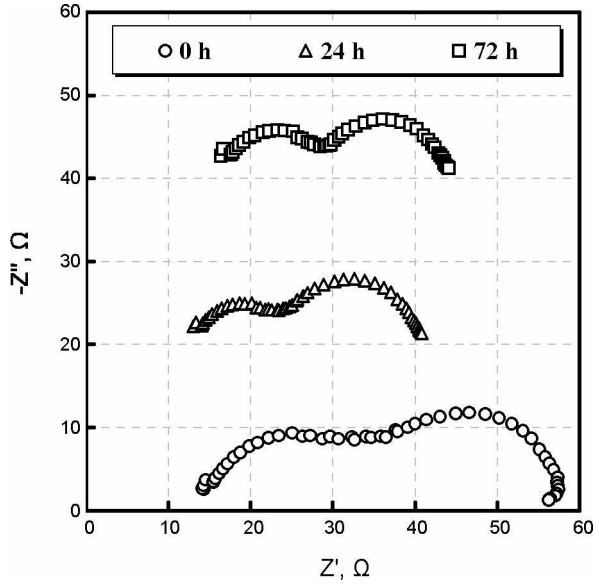

Figure 6. Nyquist plots of calcined SN-TiO_2 thin film at aging time of 40 °C.

trolyte interface decreased with increasing aging times, which result from the particle size and surface morphology as shown in Figures 5 (a, b). This result implies that the electron transport in the rutile layer is slower than in the anatase layer.[16] Similar results were reported in our preliminary studies that electron diffusion coefficient (D_n) for the rutile film is about one order of magnitude lower than that of the anatase film.

Determination of Optimal Condition for High Efficient DSSCs

The optimal condition for the highest efficiency of DSSCs

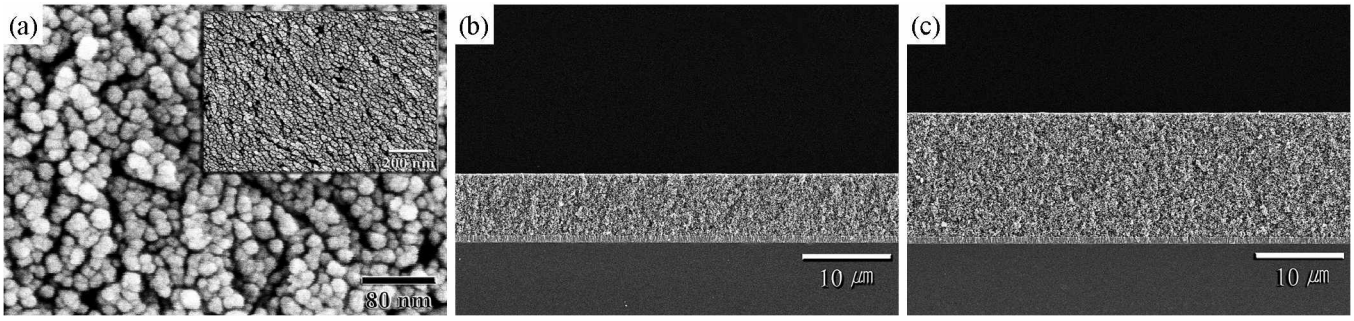

Figure 7. FE-SEM image of dried SN-TiO_2 thin film: (a) surface, (b) thickness, and (c) thickness of repetitive dry coating.

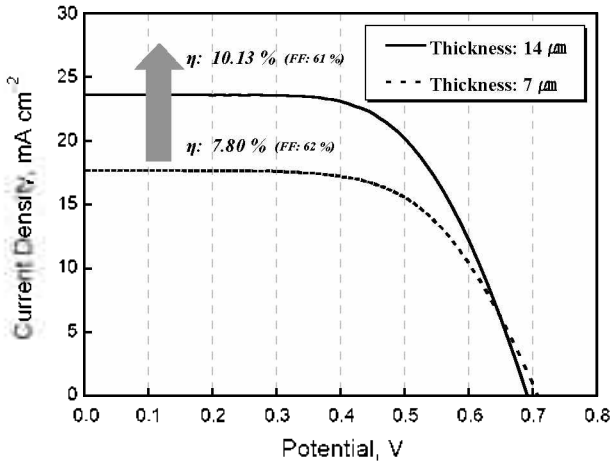

Figure 8. *I-V* curves of dried SN-TiO_2 thin films with repetitive dry coating method fabricated using TiO_2 colloidal sols prepared under optimal aging conditions of 90 °C and 72 h.

was chosen based on the experimental results. The optimal time and temperature under our experimental conditions was 72 h and 90 °C for the synthesis of TiO_2 colloidal sol. After calcination at 500 °C, TiO_2 particles mainly showed anatase phase. The average particle size was in the range of 20 nm. To increase the efficiency of DSSC with high transparency, the optimal amount of the dried SN-TiO_2 particle was determined in the range of (5 ~ 25%) and 10% of HPC as a binder. The results of conversion efficiency are listed in Table 2. Although the highest efficiency (5.16%) for 20% SN-TiO_2 sample was obtained, the fill factor was lower compared with the other samples. Thus, we reduced the TiO_2 contents from 20% to 18%. To determine the optimal amount of binder, the contents of HPC was adjusted in the range of 10 ~ 25% for the sample of 18% SN-TiO_2. As shown in Table 3, a higher conversion efficiency of 7.80% was obtained when the contents of TiO_2 and HPC were 18% and 15%, respectively. Figure 6 shows the FE-SEM image of SN-TiO_2 thin film prepared from the SN-TiO_2 colloidal sol obtained under the optimal aging conditions (i.e., 72 h, 90 °C). As shown in Figure 7 (a), the dried SN-TiO_2 thin film showed small aggregated and homogeneously dispersed particles. The average particle size was about 20 nm and the thickness of thin film was about 7 μm (Figure 7 (b)). For the manufacturing of highly efficient DSSC, we coated the TiO_2 film again using the repetitive dry coating method.[17] Figure 7 (c) shows the FE-SEM image of SN-TiO_2 thin film. The thickness of SN-TiO_2 thin film is about 14 μm. On the basis of the results obtained under our experimental conditions, the maximum energy conversion efficiency was set at 10.31% (Figure 8) for the TiO_2 thin films prepared from the TiO_2 colloidal sol synthesized under the optimal aging conditions (i.e., 72 h, 90 °C).

Conclusions

TiO_2 colloidal sol was prepared through the aging process accompanied by hydrolysis/polycondensation. We found from the analysis of XRD, FT-IR and TEM that the aging step in the colloidal sol preparation is the most important in controlling the size and structure of TiO_2 particles. It was also observed surprisingly that the physical and chemical properties of the TiO_2 particles was not changed even after the calcinations of TiO_2 sol. DSSC fabricated by the dried TiO_2 sol particles (18%) and HPC binder (15%) with a repetitive dry coating method, has a high conversion efficiency of 10.31% with high transparency.

Acknowledgments. This work was supported by the Korea Research Foundation Grant funded by the Korean Government (MOEHRD) (KRF-2007-H00023) and the Korea Institute of Geoscience and Mineral Resources of South Korea.

References

1. Hagfeldt, A.; Grätzel, M. *Acc. Chem. Res.* **2000**, *33*, 269.
2. Hwang, K. J.; Yoo, S. J.; Jung, S. H.; Park, D. W.; Kim, S. I.; Lee, J. W. *Bull. Korean Chem. Soc.* **2009**, *30*(1), 172.
3. Kang, M. G.; Ryu, K. S.; Chang, S. H.; Park, N. G.; Hong, J. S.; Kim, K. J. *Bull. Korean Chem. Soc.* **2004**, *25*(5), 742.
4. Yin, H.; Wada, Y.; Kitamura, T.; Sumida, T.; Hasegawa, Y.; Yanagida, S. *J. Mater. Chem.* **2002**, *12*, 378.
5. Park, S. D.; Cho, Y. H.; Kim, W. W.; Kim, S. J. *J. Solid State Chem.* **1999**, *146*, 230.
6. Wang, C. C.; Ying, J. Y. *Chem. Mater.* **1999**, *11*, 3113.
7. Barbe, C. J.; Arendse, F.; Comte, P.; Jirousek, M.; Lenzmann, F.; Shklover, V.; Grätzel, M. *J. Am. Ceram. Soc.* **1997**, *80*(12), 3157.
8. Jung, H. S.; Lee, S. W.; Kim, J. Y.; Hung, K. S.; Lee, Y. C.; Ko, K. H. *J. Colloid Interface Sci.* **2004**, *279*, 479.
9. Yoldas, B. E. *Amer. Ceram. Soc. Bull.* **1975**, *54*(3), 289.
10. Hwang, K. J.; Yoo, S. J.; Kim, S. S.; Kim, J. M.; Shim, W. G.; Kim, S. I.; Lee, J. W. *J. Nanosci. and Nanotechnol.* **2008**, *8*, 4976.
11. Brinker, C. J.; Scherer, G. W. *Sol-Gel Science*; Academic press: San Diego, U. S. A., 1990; p 362.
12. Yoo, S. J.; Lee, S. I.; Kwak, D. H.; Kim, K. G.; Hwang, K. J.; Lee, J. W.; Hwang, U. Y. H.; Park, H. S.; Kim, J. O. *Korean J. Chem. Eng.* **2008**, *25*(5), 1232.
13. Lee, J. W.; Hwang, K. J.; Shim, W. G.; Park, K. H.; Gu, H. B.; Kwun, K. H. *Korean J. Chem. Eng.* **2007**, *24*(5), 847.
14. Lee, J. W.; Hwang, K. J.; Park, D. W.; Park, K. H.; Shim, W. G.; Kim, S. C. *J. Nanosci. and Nanotechnol.* **2007**, *7*, 3717.
15. Park, D. W.; Park, K. H.; Lee, J. W.; Hwang, K. J.; Choi, Y. K. *J. J. Nanosci. and Nanotechnol.* **2007**, *7*, 3722.
16. Park, N. G.; van de Lagemaat, J.; Frank, A. J. *J. Phys. Chem. B* **2000**, *104*, 8989.
17. Ito, S.; Kitamura, T.; Wada, Y.; Anagida, S. *Sol. Energy Mater. Sol. Cells* **2003**, *76*, 3.